Published in IET Communications
Received on 16th March 2013
Revised on 9th August 2013
Accepted on 4th October 2013
doi: 10.1049/iet-com.2013.0218

ISSN 1751-8628

Analysis of an opportunistic large array line network with Bernoulli node deployment

Syed Ali Hassan[1], *Mary Ann Ingram*[2]

[1]*School of Electrical Engineering and Computer Science, National University of Sciences and Technology (NUST), Islamabad 44000, Pakistan*
[2]*School of Electrical and Computer Engineering, Georgia Institute of Technology, Atlanta, GA 30332, USA*
E-mail: ali.hassan@seecs.edu.pk

Abstract: A linear multi-hop cooperative network is considered where the relay nodes are deployed in a random fashion according to a Bernoulli random process. The transmission from one hop to another is modelled as a discrete-time Markov process while taking into account the random locations of the participating nodes along with the Rayleigh fading channel model. Quasi-stationary theory of Markov chains has been applied to study the various properties of the network under consideration, including successful probability of hops as well as network coverage. It is shown that there is a loss of one-hop success probability when the random deployment is done compared to a regular deployment. However, an additional signal-to-noise ratio margin has also been quantified for obtaining a desired quality of service and one-hop success probability.

1 Introduction

The opportunistic large array (OLA) is a group of single-antenna radios that transmit the same message approximately simultaneously, using any variety of transmit diversity methods, in response to a packet received from another radio or OLA [1]. An OLA is a simple but fast and reliable form of cooperative transmission (CT) or virtual array. OLAs have the characteristic that the number of cooperators or members of the group cannot be known in advance, because in the simplest case, nodes participate in an OLA if they are able to decode a packet (e.g. by passing the CRC check) and if they have not relayed that packet before. OLAs can be used for broadcasting or unicasting in a multi-hop *ad hoc* network [2–4]. If the network itself is in the form of a line of nodes, the data can be propagated down the line via a succession of OLAs. This paper studies the reliability of multiple OLA hops down a line route or network, when the nodes on the line are not equally spaced.

Linear *ad hoc* networks find a variety of applications in practical scenarios. Typical examples include structural health monitoring of buildings where the nodes are located in hallways or walls in a linear fashion, however, may not be equally spaced [5]. One-dimensional sensor networks along bridges provide another application area in addition to fault recognition in transmission lines for future smart grid systems. Another important area of application is vehicular *ad hoc* networks (VANETS), where a spatially random distribution of vehicles is formed along a road with sensors embedded in each of the vehicle [6]. A one-dimensional analysis of *ad hoc* networks can also be used to monitor road activity by spreading the spatially separated radios. Furthermore, a linear OLA network can be studied as a prelude to analyse more general two-dimensional OLA networks for designing algorithms such as routing [7, 8] and finding multi-hop distances in one and two dimensions [9].

The OLA line network can be an OLA route, which is a subset of nodes within a larger network that supports multi-OLA hopping between a source–destination pair [10]. To maintain OLA synchronisation [11], the nodes in an OLA must relay a packet quickly after receiving it, which implies the route must be set up in advance. Various methods for setting up an OLA route have been proposed, including OLAROAD [12] and OLACRA [13] protocols, the Barrage network [14] and geographical routing [15]. A demonstration of OLA transmission down a line network in a hallway can be found in [10]. Conventional (non-CT) route set-up procedures could also be used to set up an OLA route. For example, the route request and route reply phases of the *ad hoc* on-demand vector (AODV) routing protocol [16] could be used to set up the route, and then a succession of OLAs could be used for the data phase. All of the above cited studies involve nodes that are not equally spaced.

To our knowledge, no link layer error control exists for multi-hop OLA transmission, so OLA routes have only end-to-end error control [10, 14]. Link layer error control, like the retransmission protocols that are found in other wireless networks, for example, 802.11, is difficult because OLAs require no cluster heads and OLA links are inherently asymmetrical. The asymmetry follows from the fact that demodulation is done independently in each receiver, and each receiver is impacted by a different set of channel gains. Therefore, it is reasonable for us to assume no link layer retransmissions, and take an end-to-end route evaluation approach in this paper.

A variety of papers have appeared about the theory of OLA transmission. Many papers assume an infinite node density while the transmit power remains constant per unit area. This continuum of nodes assumption does not satisfy low density networks. Infinite broadcast conditions have been derived in [2, 17] under a deterministic channel model. Many results are derived with Monte Carlo simulations of the network because of increased number of modelling uncertainties. Another approach in broadcast analysis of large networks was studied in [18]. The authors have shown that there is zero probability of an infinite broadcast over a finite density extended network and the broadcast region depends on the path loss exponent of the underlying channel. In [19], the authors studied a finite density OLA line network with equally spaced nodes incorporating the fading channel in the transmission model. The upper bounds on the coverage of the network were derived given a transmit power and a required quality of service. A co-locating groups of nodes topology is studied in [20], where the OLAs form co-located clusters and a cluster-to-cluster transmission is studied. However, the clusters were at a deterministic distance from one another.

In this paper, we study the case of an extended network in which the nodes are randomly deployed over a line and complement the findings of [18] that an infinite broadcast is not possible over finite density networks. However, as opposed to [18], we quantify the coverage aspects of this network under given channel conditions. The channel model includes path loss with an arbitrary exponent and independent Rayleigh fading. The increased number of states, due to the Bernoulli deployment, necessitated a formulation in terms of Kronecker products, which greatly simplifies the analysis and the number of computations required to compute the transition matrix. The new modelling allows us to quantify the SNR loss for random node placement, relative to the regular node placement case, for different placement possibilities.

The rest of the paper is organised as follows. In the next section, we outline the system in terms of network parameters. Section 3 discusses the proposed Markov chain model and the theory of quasi-stationarity for irreducible matrices. The derivations of the transition probability matrix is descried in Section 4, while the results and network performance are stated in Section 5. The paper then concludes with future directions and recommendations in Section 6.

2 System model

Consider a decode-and-forward (DF) relaying system with nodes spatially distributed on a line. As shown in Fig. 1,

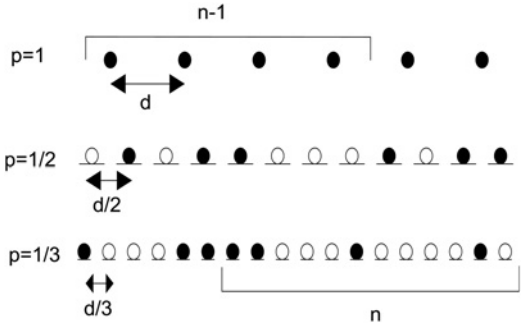

Fig. 1 *Deterministic and random placement of nodes*

our deployment model is to place nodes according to a Bernoulli process on equally spaced candidate locations, such that at most one node can be placed at a location. In other words, for every candidate location, a Bernoulli random variable $\mathcal{B}$ has the outcome $\mathcal{B} = \mathbf{1}$ with probability p if a node is present, and $\mathcal{B} = \mathbf{0}$ with probability $1 - p$, if the node is not present. We wish to compare line networks with the same average density of nodes, but with different degrees of randomness and spatial granularity. If p is a very small number, this Bernoulli deployment can be considered to be an approximation to a Poisson point process (PPP). In Fig. 1, the $p = 1$ case shows a deterministic deployment of nodes with a fixed density. We assume that the node locations are integer multiples of d, where d is the inter-node distance on the one-dimensional grid. The subsequent plots in Fig. 1 show the examples of possible Bernoulli deployments with $p = 1/2$ and $p = 1/3$, respectively. The filled-in circles indicate the existence of a node whereas the hollow circles show the absence of a node. Thus, p can be regarded as the granularity parameter where smaller values of p corresponds to higher granularity. As $p \to 0$, the resulting deployment follows a PPP. Although for a random network, a PPP is generally used as a stochastic model, however, the PPP approach is sometimes not a valid assumption [21]. This is because usually there is a finite and fixed number of nodes in a network and these fixed nodes are scattered in a pre-defined area or volume, hence a binomial point process can often lead to more realistic scenario where a fixed number of nodes are placed in a fixed area. Each node can be placed at a particular location with a certain success probability, defining a Bernoulli process, as modelled in this paper.

For all cases, we assume that cooperating nodes transmit synchronously in OLAs or levels. Specifically, we assume that a group of nodes in the vicinity of each other constitute a level and all the nodes of that level transmit the same message to all the nodes of adjacent (next) level providing transmit diversity. Diversity in this network can be achieved by transmitting the same message through orthogonal fading channels, for instance by employing frequency diversity or using a suitable space–time code. We do not explicitly address the formation of orthogonal channels in this paper other than to suggest that in a line network a repetitive code can be used, such that the code length is at least as long as the hop distance. A successful hop occurs when nodes in one level transmit a message and at least one node, in the forward direction, is able to decode the message for the first time. Correct decoding is assumed when a node's received SNR at the output of the diversity-combiner, from the previous level only, is greater than or equal to a modulation-dependent threshold, τ. Exactly one time slot later, all the nodes that just decoded the message relay the message and this process continues. Once a node has relayed a message, it will not relay that message again. We assume that a level can have a finite region of support of width M and the hop distance between two successive levels is given as h_d. Hence h_d can be considered as a shift to the window of size M, on the reference deterministic case. The horizontal square brackets in Fig. 1 show an example of adjacent window positions, corresponding to $M = 4$ and hop distance $h_d = 2$. We assume that all the nodes transmit with the same transmit power P_t. A node receives superimposed copies of the message signal from the nodes that decoded the message correctly in the previous level, over orthogonal fading channels using maximum ratio combining. Let us define

doi: 10.1049/iet-com.2013.0218

$\mathbb{N}_n = \{1, 2, \ldots, k_n\}$, where k_n is the cardinality of the set $\mathbb{N}_n$ such that $\sup_n k_n \leq M$, to be the set of slot indices of those nodes that decoded the signal perfectly at the time instant (or hop) n. The received power at the jth node at the next time instant $n+1$ is given by

$$P_{r_j}(n+1) = \frac{P_t}{d^\beta} \sum_{m \in \mathbb{N}_n} \frac{\mu_{mj}}{|h_d - m + j|^\beta} \tag{1}$$

where the summation is over the nodes that decoded correctly in the previous level. We note that (1) also represents the received power for equal gain combining in a non-coherent receiver [11]. Here d denotes the inter-node distance for $p = 1$. For other values of granularity, we use corresponding values of distance as shown in Fig. 1. Similarly, the hop distance h_d is also a function of granularity level, for example, $h_d = 2$ for $p = 1$ and $h_d = 4$ for $p = 1/2$ in Fig. 1. The flat fading Rayleigh channel gain from node m in the previous level to node j in the current level is denoted by μ_{mj}, where the gains of the different node pairs are independently and identically distributed (i.i.d.) and are drawn from an exponential distribution with the parameter $\sigma_\mu^2 = 1$; β is the path loss exponent with a usual range of 2–4. Consequently, the received SNR at the jth node is given as $\gamma_j = P_{r_j}/\sigma^2$, where σ^2 is the variance of the noise in the receiver. We assume perfect timing and frequency recovery at each receiver, and we also assume that there is sufficient transmit synchronisation between the nodes of a level, such that all the nodes in a level transmit to the next level at the same time [11]. In other words, the transmissions only occur at discrete instants of time, n, $n+1$,…, such that the hop number and the time instants can be defined by just one index n.

3 Markov model

At a certain hop number n, a node, if present at a slot, will take part in the next transmission, if it has decoded the data perfectly for the first time, or it will not take part, if it did not decode correctly or it has already decoded the data in one of the previous levels. The states of all the slots in the nth level can be represented as $\mathcal{X}(n) = [\mathbb{I}_1(n), \mathbb{I}_2(n), \ldots, \mathbb{I}_M(n)]$, where $\mathbb{I}_j(n)$ is the ternary indicator random variable for the jth slot at the nth time instant given as

$$\mathbb{I}_j(n) = \begin{cases} 0, & \text{slot } j \text{ has a node, which has not decoded} \\ 1, & \text{slot } j \text{ has a node, which has decoded} \\ 2, & \text{slot } j \text{ has no node or it has} \\ & \text{a node that has decoded at some earlier time} \end{cases} \tag{2}$$

Thus, each slot in a level is represented by either 0, 1 or 2 depending upon node presence and successful decoding of the received data. We observe that the outcomes of $\mathcal{X}(n)$ are ternary M-tuples, each outcome constituting a state, and there are 3^M number of states, which are enumerated in decimal form 0, 1, …, $3^M - 1$, then we may write

$$\begin{aligned} &\mathbb{P}\{\mathcal{X}(n) = i_n | \mathcal{X}(n-1) = i_{n-1}, \ldots, \mathcal{X}(1) = i_1\} \\ &= \mathbb{P}\{\mathcal{X}(n) = i_n | \mathcal{X}(n-1) = i_{n-1}\} \end{aligned} \tag{3}$$

where $\mathbb{P}$ indicates the probability measure. Equation (3) implies that $\mathcal{X}$ is a discrete-time finite-state Markov process. Assuming the statistics of the channel are the same for all the hops in the network, the Markov chain can be regarded as a homogeneous one. Absorption in the Markov chain occurs when a state comprises any combination of 0 and 2 s. Hence, we consider the Markov chain, $\mathcal{X}$, on a state space $\mathcal{A} \cup \mathcal{S}$, where $\mathcal{S}$ is a set of transient states and $\mathcal{A}$ is the set of absorbing states, and we have

$$\lim_{n \to \infty} \mathbb{P}\{\mathcal{X}(n) \in \mathcal{A}\} \nearrow 1 \quad \text{a.s.} \tag{4}$$

To make the irreducible transition matrix, we strike the rows and columns corresponding to transitions to and from the absorbing states. Note that the transition matrix is square, irreducible, non-negative and right sub-stochastic. We therefore, invoke the Perron Frobenious theorem [22] which states that, there exists a unique maximum eigenvalue, ρ, such that the eigenvector associated with ρ is unique and has strictly positive entries, where $0 < \rho < 1$. Since $\forall n$, $\mathbb{P}\{\mathcal{X}(n) \in \mathcal{A}\} > 0$, eventual killing is certain. We let $T = \inf\{n \geq 0 : \mathcal{X}(n) \in \mathcal{A}\}$ denote the end of the survival time, that is, the time at which killing occurs. It follows then

$$\mathbb{P}\{T > n + m | T > n\} = \rho^m \tag{5}$$

while the quasi-stationary distribution of the Markov chain is given as [23]

$$\lim_{n \to \infty} \mathbb{P}\{\mathcal{X}(n) = j | T > n\} = u_j, j \in S \tag{6}$$

4 Transition probability matrix

For finding the state transition matrix for our model, we split our analysis into two subsections. The first subsection deals with finding the one-step transition probability of transiting from one state to another. In the next subsection, we formulate the ways in which the matrix could be obtained without explicitly calculating each transition and hence the algorithm is made less computationally complex. One goal of this study is to find the hop distance as a function of the values of system parameters such as relay transmit power and inter-node distance. However, because of the discrete nature of the hop distance, solving the problem is this manner is quite tedious. Hence in this paper, we follow the inverse approach, that is, for a given hop distance, we will find the system parameters that generate this hop distance. Therefore, we assume a fixed M and h_d in designing the one-step transition probability matrix.

4.1 Formation of the one-step transition probability

Let i and j denote a pair of states of the system such that $i, j \in \mathcal{S}$, where each i and j are the decimal equivalents of the ternary words formed by the set of indicator random variables. To determine the possible destination states in a transition from level $n-1$ to level n, it is helpful to distinguish between two mutually exclusive sets of nodes at the nth level: (i) the nodes that were also in the M-slot window of the $(n-1)$th level, that is, nodes that are in the $M - h_d$ overlap region of the two consecutive windows, and (ii) the remaining h_d nodes that are not in the overlap

Fig. 2 *State diagram of a single slot*

region. We denote these two sets of nodes as $\mathbb{N}_{\mathrm{OL}}^{(n)}$ and $\overline{\mathbb{N}}_{\mathrm{OL}}^{(n)}$, respectively, where OL stands for overlap.

Suppose node k in $\mathbb{N}_{\mathrm{OL}}^{(n)}$ decoded in the previous $(n-1)$th level; this would be indicated by $\mathbb{I}_{h_d+k}(n-1)=1$. This node will not decode again, and therefore $\mathbb{I}_k(n)=2$. Similarly, if that node decoded prior to the $(n-1)$th level, or if there were no node in the kth slot of $(n-1)$th level, then $\mathbb{I}_{h_d+k}(n-1)=2$. In this case also, we must have $\mathbb{I}_k(n)=2$. Alternatively, if the node is present and has not previously decoded, then $\mathbb{I}_{h_d+k}(n-1)=0$, and $\mathbb{I}_k(n)$ can equal 0 or 1, depending on the previous state and the channel outcomes; $\mathbb{I}_k(n)=2$ is not possible. If the location k is in the $\overline{\mathbb{N}}_{\mathrm{OL}}^{(n)}$, then there is no previous level index for this node, and we can have $\mathbb{I}_k(n)\in\{0,1,2\}$ depending on the node presence, previous state and channel outcomes. Hence from this discussion and (2), we note that a slot can have three possible states. Hence each individual slot is a state machine, and $\mathbb{I}_k(n)$ is generally a non-homogeneous Markov chain itself; the probabilities of transition for a single node are non-zero only at certain times. This slot Markov chain is depicted in Fig. 2.

Let the superscript on an indicator function show the state associated with that indicator function. For example, if $i=22110$, then $\mathbb{I}_5^{(i)}(n)=0$. Therefore, considering the above discussion, the one-step transition probability going from the state i in level $n-1$ to state j in level n is always 0, $\forall k=0,1,2,\ldots,M$, when either of the following conditions is true

$$\text{Condition I:}\mathbb{I}_k^{(j)}(n)\in\{0,1\}\text{ and }\mathbb{I}_{h_d+k}^{(i)}(n-1)\in\{1,2\} \tag{7}$$

$$\text{Condition II:}\mathbb{I}_k^{(j)}(n)=2\text{ and }\mathbb{I}_{h_d+k}^{(i)}(n-1)=0 \tag{8}$$

In the following, we assume that the previous state is a transient state; that is, $\mathcal{X}(n-1)\in\mathcal{S}$. For each node $k\in\mathbb{N}_{\mathrm{OL}}^{(n)}$, the probability of being able to decode at time n given that the node exists but failed to decode in the previous level (P_{01} from Fig. 2) is given as

$$\begin{aligned}&\mathbb{P}\left\{\mathbb{I}_k^{(j)}(n)=1\middle|\mathbb{I}_{h_d+k}^{(j)}(n-1)=0,\,\mathcal{X}(n-1)\right\}\\&=\left\{\gamma_k(n)>\tau\middle|\mathbb{I}_{h_d+k}^{(j)}(n-1)=0,\,\mathcal{X}(n-1)\right\}\end{aligned} \tag{9}$$

If $k\in\overline{\mathbb{N}}_{\mathrm{OL}}^{(n)}$, and $\mathcal{V}_{\overline{\mathrm{OL}}}$ is the cardinality of set $\overline{\mathbb{N}}_{\mathrm{OL}}^{(n)}$, then we define a sequence of Bernoulli random variables $\mathcal{B}(n)$ such that $\mathcal{B}(n)=\left\{\mathcal{B}_1(n),\mathcal{B}_2(n),\ldots,\mathcal{B}_{\mathcal{V}_{\overline{\mathrm{OL}}}}(n)\right\}$, and also denote the event $\left\{\mathbb{I}_{h_d+k}^{(j)}(n-1)=0,\mathcal{X}(n-1),\mathcal{B}_k(n)=1\right\}$ as ξ, then

$$\begin{aligned}&\mathbb{P}\left\{\mathbb{I}_k^{(j)}(n)=1\middle|\mathbb{I}_{h_d+k}^{(j)}(n-1)=0,\,\mathcal{X}(n-1)\right\}\\&=\mathbb{P}\{\gamma_k(n)>\tau|\xi\}\mathbb{P}\{\mathcal{B}_k(n)=1\}\end{aligned} \tag{10}$$

and

$$\mathbb{P}\left\{\mathbb{I}_k^{(j)}(n)=2,\mathcal{B}_k(n)=0\right\}=\mathbb{P}\{\mathcal{B}_k(n)=0\} \tag{11}$$

Also

$$\mathbb{P}\{\gamma_k(n)>\tau|\xi\}=\int_\tau^\infty p_{\gamma_k|\xi}(y)\mathrm{d}y \tag{12}$$

$p_{\gamma_k|\xi}(y)$ is the conditional probability density function (PDF) of the received SNR at the kth node, conditioned on state $\mathcal{X}(n-1)$ and the node existing but not having decoded yet, and is given by the hypoexponential distribution [19]. For the formulation of one step transition probability from state i to state j, define

$$\mathbb{N}_{\theta_{\mathrm{OL}}}^{(j)}=\left\{k{:}k\in\mathbb{N}_{\mathrm{OL}}^{(n)},\mathbb{I}_k^{(j)}(n)=\theta\right\},\quad\theta\in\{0,1\}$$

$$\mathbb{N}_{\theta_{\overline{\mathrm{OL}}}}^{(j)}=\left\{k{:}k\in\overline{\mathbb{N}}_{\mathrm{OL}}^{(n)},\mathbb{I}_k^{(j)}(n)=\theta\right\},\quad\theta\in\{0,1,2\}$$

and let $\mathcal{V}_\theta$ be the cardinality of $\mathbb{N}_{\theta_{\overline{\mathrm{OL}}}}^{(j)}$, $\theta\in0,1,2$. Then the one step transition probability for going from state i to state j is 0 if Condition I or II holds, otherwise it is given as

$$\begin{aligned}\mathbb{P}_{ij}=&\prod_{k\in\mathbb{N}_{1_{\mathrm{OL}}}^{(j)}}\left(\psi_m^{(k)}\right)\prod_{k\in\mathbb{N}_{1_{\overline{\mathrm{OL}}}}^{(j)}}\left(\psi_m^{(k)}\right)(p)^{\mathcal{V}_1}\\&\times\prod_{k\in\mathbb{N}_{0_{\mathrm{OL}}}^{(j)}}\left(1-\psi_m^{(k)}\right)\prod_{k\in\mathbb{N}_{0_{\overline{\mathrm{OL}}}}^{(j)}}\left(1-\psi_m^{(k)}\right)(p)^{\mathcal{V}_0}\left(1-p\right)^{\mathcal{V}_2}\end{aligned} \tag{13}$$

where $\psi_m^{(k)}$ is the probability of success of node k in level n and is given as

$$\psi_m^{(k)}=\sum_{m\in\mathbb{N}_{n-1}}C_m^{(k)}\exp\left(-\lambda_m^{(k)}\tau\right) \tag{14}$$

where $\mathbb{N}_{n-1}=\left\{m{:}\mathbb{I}_m^{(i)}(n-1)=1\right\}$ was previously defined as the set of the slot indices of all those nodes that decoded the data perfectly in the previous level, $\lambda_m^{(k)}$ is given as

$$\lambda_m^{(k)}=\frac{d^\beta\left|h_d-m+k\right|^\beta\sigma^2}{P_t} \tag{15}$$

and $C_m^{(k)}$ is defined as

$$C_m^{(k)}=\prod_{\zeta\neq m}\frac{\lambda_\zeta^{(k)}}{\lambda_\zeta^{(k)}-\lambda_m^{(k)}} \tag{16}$$

Equation (13) gives just a single entry of the transition matrix for two given states of the system. Similar entries for all $i,j\in S$ can be computed to form the transition probability matrix.

4.2 Kronecker representation of the transition matrix

Many transition probabilities, $\mathbb{P}_{ij}$, in (13), are zero and hence the transition probability matrix is sparse. Rather than computing each non-zero element separately, the Kronecker representation can enable obtaining the same matrix with fewer computations.

The total number of states in the model is 3^M, where we may enumerate the state space as decimal equivalents of the

doi: 10.1049/iet-com.2013.0218

ternary M-tuples, that is, 0, 1, …, $3^M - 1$; hence the transition matrix, $\boldsymbol{P}$, can be partitioned into three rectangular blocks as $\boldsymbol{P} = [\boldsymbol{P}_0^{(1)} \quad \boldsymbol{P}_1^{(1)} \quad \boldsymbol{P}_2^{(1)}]^{\mathrm{T}}$, where T denotes the block transpose, such that the most significant symbol (MSS) in the ternary expansion of ith row of matrices $\boldsymbol{P}_0^{(1)}$, $\boldsymbol{P}_1^{(1)}$ and $\boldsymbol{P}_2^{(1)}$ is 0, 1 and 2, respectively. In all the cases, the superscript (1) shows that we are dealing with the MSS. This procedure is shown in Fig. 3, where the ternary expansion of some states are shown for $M = 4$.

Also note that the contribution to the received power at any node in the current level, n, is zero if the originating state corresponding to that MSS was either 0 or 2 in the previous level, $n-1$. For instance, if the previous state was 0110, the received power at any node in the next level remains the same even if the previous state was 2110. This is because only the nodes which are in state 1 are contributing to the received power. This results in equal probability of transition to a given state, if the originating state's MSS is 0 or 2. Thus, the transition probabilities to all of the 3^M states from states with MSS = 0, 2 are equal, since no power is originating from these MSS. Thus, if i represents all states with 0 MSS and j represents all the states with 2 MSS, then all transitions from i and j results in equal probability numbers. Hence $\boldsymbol{P}_0^{(1)} \equiv \boldsymbol{P}_2^{(1)}$. If the dimension of $\boldsymbol{P}$ is $\dim(\boldsymbol{P}) = 3^M \times 3^M$, then $\dim(\boldsymbol{P}_\alpha^{(1)}) = 3^{M-1} \times 3^M$, $\forall \alpha = \{0, 1, 2\}$. Hence, we can write

$$\boldsymbol{P} = \begin{bmatrix} 1 \\ 0 \\ 1 \end{bmatrix} \otimes \boldsymbol{P}_0^{(1)} + \begin{bmatrix} 0 \\ 1 \\ 0 \end{bmatrix} \otimes \boldsymbol{P}_1^{(1)} = \begin{bmatrix} \boldsymbol{P}_0^{(1)} \\ \boldsymbol{P}_1^{(1)} \\ \boldsymbol{P}_0^{(1)} \end{bmatrix} \tag{17}$$

where $\otimes$ denotes the Kronecker or tensor product. Thus, the explicit computation of $\boldsymbol{P}_2^{(1)}$ is not required. The representation in (17) is depicted for the case when the first slot in the previous level was either 0 or 2. Similarly, for the next location in the previous level, each of the $\boldsymbol{P}_\alpha$s are further divided into a set of three matrices, as shown in Fig. 3, depending on the state of second slot being 0 or 2, and this process of splitting matrices into a ternary tree goes on for all locations m in level $(n-1)$ such that $m = \{1, 2, \ldots, h_d\}$. If $V_0 := [1 \quad 0 \quad 1]^{\mathrm{T}}$, and $V_1 := [0 \quad 1 \quad 0]^{\mathrm{T}}$,

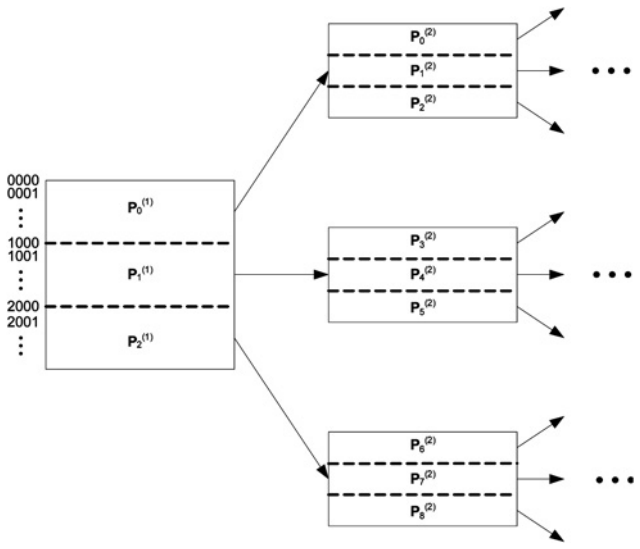

Fig. 3 *Ternary decomposition of the transition matrix*

then a compact representation of $\boldsymbol{P}$ is given as

$$\boldsymbol{P} = \sum_{\alpha=0}^{2^{h_d}-1} \left[\left(\otimes_{j=0}^{h_d-1} V_{\alpha_j} \right) \otimes \boldsymbol{P}_\alpha^{(h_d)} \right] \tag{18}$$

where $\alpha_j \in 0, 1$ is the jth digit in the binary expansion of α, such that $\alpha = \sum_{j=0}^{h_d-1} 2^j \alpha_j$. For each α, the $\dim(\boldsymbol{P}_\alpha^{(h_d)}) = 3^{M-h_d} \times 3^M$, which is far less than that of dim ($\boldsymbol{P}$) itself for a large h_d. In other words, if 3^{2M} computations are required to find $\boldsymbol{P}$, then by using (18), $(2/3)^{h_d} 3^{2M}$ computations are required, which are fewer computations by a factor of $(2/3)^{h_d}$. Since from Fig. 1, we need more slots per hop for smaller granularity, the representation in (18) is helpful. For example, if hop distance is 6 and window size is 10, then by using the above representation, we have to perform only 8.77% of the calculations as compared to calculating the full matrix $\boldsymbol{P}$. Also note that the total states are 3^M; however $|\mathcal{S}| = 3^M - 2^M$, where $|\mathcal{A}| = 2^M$ is the number of absorbing states. Hence the computations are further reduced. It has also been observed that the matrix is highly sparse due to conditions derived in (7) and (8). For example, for the aforementioned case, the resulting matrix is more than 98% sparse. Hence for the purpose of modelling, we can use these simplifications to reduce the computational complexity. The representation in (18) is used to derive the transition matrix with a large number of states and is called the stochastic automata network (SAN) descriptor [24]. If large window sizes and hop distances must be evaluated, then there exist methods like GMRES and Arnoldi iterations that make use of this SAN representation to find the eigenvalues and the probability vector for the transition probability matrix. Interested readers can see, for instance, [25] (and the references therein), where the problem of state space explosion is studied and solved using the SAN representation and iterative methods.

5 Results and system performance

In Section 3, we showed how the transition matrix is fully characterised by its Perron eigenvalue and the corresponding left eigenvector, which gives the quasi-stationary distribution of the chain. However, the Perron eigenvalue, which is the one-OLA-hop success probability in our case, depends upon many parameters like transmit power, path loss exponent, inter-slot distance and so on. Hence an infinite solutions can be obtained by changing the values of these parameters. To decrease the design space dimension, we observe that the transition matrix, from (13) and (14), depends on the product $\lambda_m^{(k)}\tau$, from which we can extract the normalised parameter

$$\Upsilon = \frac{\gamma_0}{\tau} = \frac{P_t}{d^\beta \sigma^2} \frac{1}{\tau} \tag{19}$$

which can be interpreted as the SNR margin at a receiver from a single transmitting node, a distance d away. However, Υ is not the only independent parameter, because β and h_d also separately impact the value of $\lambda_m^{(k)}\tau$ in (15), through the factor $|h_d - m + k|^\beta$ and $\mathbb{P}_{ij}$ also depends upon the granularity level p.

In the following, we will discuss the case depicted in Fig. 1, that is, a mean hop distance of 2 and its corresponding different network topologies with random placement and

path loss exponent of 2. Similar results and analysis can be done for other topologies. The mean hop distance refers to the hop distance in the deterministic deployment. Note that the window size, M, is one of the factors that affects the values of ρ and the model space dimension. M is an artificial constraint because there is no real physical need for it, however, it strongly impacts the size of the state space and therefore the computational complexity of finding the success probability. Therefore, we would like for M to be as small as possible without significantly impacting the system performance results. As in [19], we propose to find M by increasing the window size for a given hop distance, until the one-hop success probability (i.e. the Perron–Frobenius eigenvalue, ρ) ceases to change significantly. This implies that even if we add another slot at the forward edge of the window, there is no or little effect on the success probability because the transmissions reaching that specific slot are attenuated owing to the large path loss. Fig. 4 depicts the trend of eigenvalues as we increase the SNR margin for different window sizes and a mean hop distance of 2 with $p = 1/2$. The behaviour is quite obvious that increasing SNR margin increases the probability of survival of the transmissions. It can be further noticed that for a given value of SNR margin, the curves start to converge as we increase the window size, thereby indicating that after a specific window size, even if we increase M, there is no change in the transmissions outcome. Thus, we select the window size where this convergence is achieved.

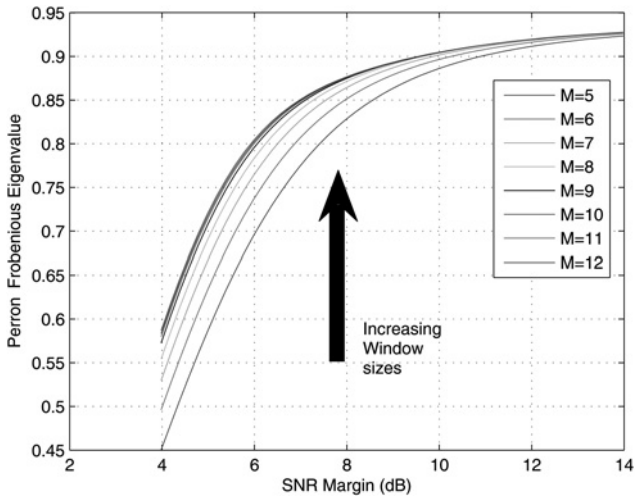

Fig. 4 *Behaviour of success probabilities with the increase in window size for a mean hop distance of 2*

To compare the SNR margin required for a given quality of service, which can be the one-hop success probability in this case, the behaviour of success probability is plotted against SNR margin for different granularity levels in Fig. 5. In all cases, the mean hop distance is 2. Thus, it can be seen that a smaller SNR margin is required to get the same success probability for deterministic deployment as compared to the random deployment. For example, for 85% success probability, the deterministic deployment requires 5.55 dB of the SNR margin, whereas the SNR margins required are 7.1, 8.5 and 10 dB for $p = 1/a$, $a = \{2, 3, 4\}$, respectively. A similar plot is also shown for a mean hop distance of 3 in Fig. 6, where we can observe that the behaviour of curves is the same as for mean hop distance 2; however, we can achieve higher values of success probabilities as the SNR margin increases, because larger hop distance corresponds to more transmitters per hop and therefore more diversity gain. Hence, the proposed modelling gives the accurate knowledge of the success probabilities for various SNR margins and for various granularity levels. The additional SNR margin required decreases at every step as we increase the granularity level. For instance, from Fig. 6, for a 90% success probability, the SNR margins required are 7.3, 9.2 and 10 dB for $p = 1/a$, $a = \{1, 2, 3\}$, respectively. Thus, we can infer that as $p \to 0$, $\Upsilon \to \tilde{\Upsilon}$, as a consequence of law of large numbers, where $\tilde{\Upsilon}$ specifies the convergent value of SNR margin for an infinitesimal small value of p.

The curves in Figs. 5 and 6 appear to be approaching limits as SNR increases. For $p < 1$, these apparent limits are less than one. The existence of a limit follows from the Bernoulli model of node placement; a hop failure can occur if there are no nodes available in the next-hop window of width M, which happens with probability $(1-p)^M$. Therefore, under our assumption that no node beyond that window is allowed to participate in the next hop, $1-(1-p)^M$ is an upper bound on the one-hop success probability for a fixed M. However, we found that the values of this bound, for

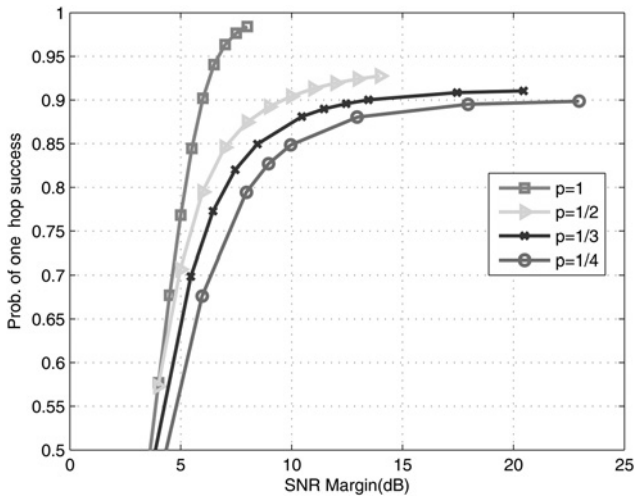

Fig. 5 *Success probabilities as a function of SNR margin for a mean hop distance of 2 and various granularity levels*

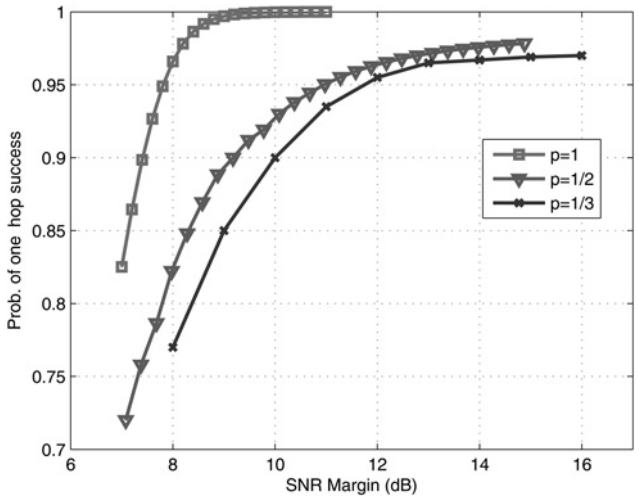

Fig. 6 *Success probabilities as a function of SNR margin for a mean hop distance of 3 and various granularity levels*

doi: 10.1049/iet-com.2013.0218

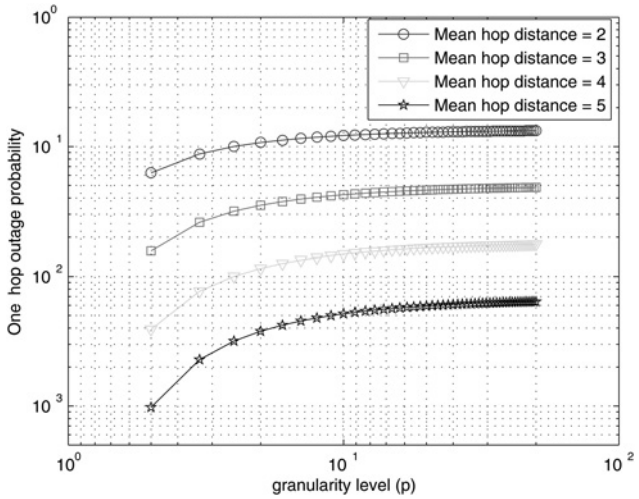

Fig. 7 *Asymptotic behaviour of success probabilities at very high SNR margin*

example, 0.997, 0.993 and 0.989 for $p = 1/2$, 1/3 and1/4, respectively. This is because of the overlapping nature of windows since the $M - h_d$ slots are already taken into account in the previous window. This bound of $1 - (1 - p)^{h_d}$ also fits on the asymptotic values in Fig. 6 for mean hop distance 3.

Fig. 7 shows the asymptotic values of the outage probability for different granularity levels. It can be observed that the outage decreases with the increase in the mean hop distance, which is because of an increased diversity gain. Let the success probability ρ, as a function of $p = 1/a$, be written as ρ_a, where $a = \{1, 2, \ldots, \infty\}$. If $\Delta\rho_a = \rho_a - \rho_{a+1}$ is defined as the sequence obtained by taking the difference of success probabilities at different granularity levels, then it can be observed from Fig. 7 that the sequence $\Delta\rho_a$ is a monotone decreasing sequence with the increasing values of a. This implies that, as $a \to \infty$, $\Delta\rho_a \to 0$, and $\rho \to \tilde{\rho}$, as a consequence of law of large numbers, where $\tilde{\rho}$ is the smallest success probability, obtained at infinite SNR, when the deployment of nodes follow the PPP. Another observation is that all the curves make a horizontal asymptote as $p \to 0$. This shows that the

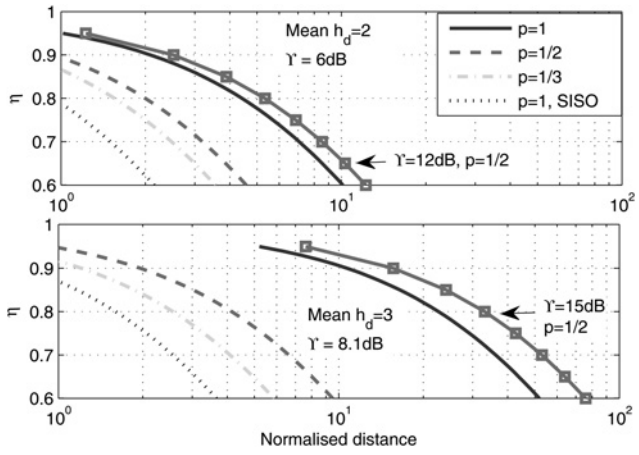

Fig. 8 *Normalised distance for given quality of service with different mean hop distances*

The squared-marker curves show the $p = 1/2$ case at an indicated higher SNR margin

Bernoulli process approaches the Poisson process in the limit and the probability of outage remains the same with further decrease in the granularity level. Hence, we observe the phenomenon of diminishing returns for ρ, which is also evident from Figs. 5 and 6. Hence, the Bernoulli deployment of nodes with relatively higher values of p, for example, $p = 1/4$ could also provide an approximate behaviour of an *ad hoc* line network.

From the deployment perspective of the network, it is sometimes desirable to determine the values of certain parameters such as transmit power of relays to obtain a certain quality of service (QoS), η. In other words, we are interested in finding the probability of delivering the message at a certain distance without having entered the absorbing state, and we desire this probability to be at least η where $\eta \sim 1$ ideally. Thus, (5) gives us a nice upper bound on the value of m (the number of hops) one can go with a given η, that is, $\rho^m \geq \eta$, which gives

$$m \leq \frac{\ln \eta}{\ln \rho} \tag{20}$$

Thus, if the destination is far off, we require more hops, which will require a larger value of ρ. Fig. 8 shows the relationship between QoS, η, and the normalised distance for different values of granularity level. The normalised distance, which is the true distance divided by d, is defined as the product of h_d and the number of hops (made to reach the destination). The upper graph corresponds to a mean hop distance, h_d, of two, while the lower graph corresponds to $h_d = 3$. In the upper graph, the four curves described in the legend have an SNR margin, ϒ, of 6 dB. One of these curves corresponds to the non-CT or single input single output (SISO) case, given for reference. To show how a higher SNR margin can overcome losses associated with $p < 1$, we have also plotted the square-marker curve for ϒ = 12 dB and $p = 1/2$. Similarly, the lower graph has four curves with ϒ = 8.1 dB and one square-marker curve with ϒ = 15 dB and $p = 1/2$. We observe that for a fixed SNR margin (i.e. not including the square-marker curves) more random deployment or higher granularity implies a shorter distance can be covered for a given QoS. At low QoS, for example, $\eta = 0.7$, the network is able to reach a particular distance with different granularity levels. Whereas, at high QoS, for example, 0.9, the highest granularities are not possible. The $p = 1$ case always gives the best coverage for all values of the quality of service. The square-marker curves show that increasing the SNR margin can compensate the 'random placement loss.' We notice that the deterministic SISO topology has very small coverage as compared to any cooperative topology with or without random deployment. We point out that retransmissions would increase the reliability of the SISO case, as well as the CT cases. However, retransmissions are quite challenging to implement in OLA-based networks, therefore we have assumed no retransmissions in this paper.

6 Conclusion

In this paper, we have shown that the quasi-stationary Markov chain model can be applied to a one-dimensional *ad hoc* network, where the nodes can be randomly placed. We have modelled the presence or absence of a node at a location using the Bernoulli process and formulated the state space of our system using indicator random variables.

We have also derived a compact tensor representation of the transition probability matrix which is based on the underlying hypoexponential distribution of the received power. The behaviour of the Perron–Frobenius eigenvalue of the sub-stochastic matrix, referred as the success probability, indicated the level of quality of service that can be achieved for a certain transmission. We have shown margin for the random placement of nodes implies a disadvantage in terms of SNR as compared to deterministic placement for the same success probability. However, this loss can be compensated by increasing the SNR margin.

7 Acknowledgment

The authors would like to thank Professor Erik Verriest for his helpful suggestion on Kronecker algebra.

8 References

1 Scaglione, A., Hong, Y.W.: 'Opportunistic large arrays: cooperative transmission in wireless multi-hop ad hoc networks to reach far distances', *IEEE Trans. Signal Process.*, 2003, **51**, (8), pp. 2082–92
2 Mergen, B.S., Scaglione, A.: 'A continuum approach to dense wireless networks with cooperation', In Proc. IEEE INFOCOM, March 2005, pp. 2755–2763
3 Mergen, B.S., Scaglione, A., Mergen, G.: 'Asymptotic analysis of multi-stage cooperative broadcast in wireless networks', *IEEE Trans. Inf. Theory*, 2006, **52**, (6), pp. 2531–2550
4 Thanayankizil, L., Kailas, A., Ingram, M.A.: 'Routing for wireless sensor networks with an opportunistic large array (OLA) physical layer', Ad Hoc and Sensor Wireless Networks, Special Issue on the 1st Int. Conf. Sensor Technologies and Applications, 2009, vol. 8, no. 1–2, pp. 79–117
5 Kim, S., Pakzad, S., Culler, D., *et al.*: 'Wireless sensor networks for structural health monitoring'. In Proc. Fourth ACM Int. Conf. Embedded Networked Sensor Systems, 2006, pp. 427–428
6 Willke, T.L., Tientrakool, P., Maxemchuk, N.F.: 'A survey of inter-vehicle communication protocols and their applications', *IEEE Commun. Surv. Tutorials*, 2009, **11**, (2), pp. 3–20
7 Behnad, A., Nader-Esfahani, S.: 'On the statistics of MFR routing in one-dimensional ad hoc networks', *IEEE Trans. Veh. Technol.*, 2011, **60**, (7), pp. 3276–3289
8 Zimmerling, M., Dargie, W., Reason, J.M.: 'Energy-efficient routing in linear wireless sensor networks'. In IEEE Int. Conf. Mobile Ad hoc and Sensor Systems, (MASS), 2007
9 Vural, S., Ekici, E.: 'Probability distribution of multi-hop-distance in one-dimensional sensor networks', *Comput. Netw.*, 2007, **51**, (13), pp. 3727–3749
10 Chang, Y.J., Jung, H., Ingram, M.A.: 'Demonstration of an OLA-based cooperative routing protocol in an indoor environment'. In 17th European Wireless Conference, Vienna, Austria, April 2011
11 Chang, Y.J., Ingram, M.A.: 'Cluster transmission time synchronization for cooperative transmission using software defined radio'. IEEE (ICC) Workshop on Cooperative and Cognitive Mobile Networks (CoCoNet3), May 2010
12 Thanayankizil, L., Ingram, M.A.: 'Reactive robust routing with opportunistic large arrays'. In Proc. IEEE ICC Workshop, June 2009
13 Thanayankizil, L., Kailas, A., Ingram, M.A.: 'Opportunistic large array concentric routing algorithm (OLACRA) for upstream routing in wireless sensor networks', *Ad Hoc Netw.*, 2011, **9**, (7), pp. 1140–1153
14 Halfold, T.R., Chugg, K.M.: 'Barrage relay networks'. In Information Theory and Applications Workshop (ITA), Feb. 2010
15 Mauve, M., Widmer, A., Hartenstein, H.A.: 'Survey on position-based routing in mobile ad hoc networks', *IEEE Network*, 2001, **15**, (6), pp. 30–39
16 Perkins, C.E., Belding-Royer, E.M., Das, S.R.: 'Ad hoc on-demand distance vector (AODV) routing'. Published Online, Internet Engineering Task Force, RFC Experimental 3561, July 2003
17 Kailas, A., Ingram, M.A.: 'Analysis of a simple recruiting method for cooperative routes and strip networks', *IEEE Trans. Wirel. Commun.*, 2010, **9**, (8), pp. 2415–2419
18 Capar, C., Goeckel, D., Towsley, D.: 'Broadcast analysis for large cooperative wireless networks'. arXiv preprint arXiv:1104.3209, 2011
19 Hassan, S.A., Ingram, M.A.: 'A quasi-stationary Markov chain model of a cooperative multi-hop linear network', *IEEE Trans. Wirel. Commun.*, 2011, **10**, (7), pp. 2306–2315
20 Hassan, S.A., Ingram, M.A.: 'Benefit of co-locating groups of nodes in cooperative line networks', *IEEE Commun. Lett.*, 2012, **16**, (2), pp. 234–237
21 Srinivasa, S., Haenggi, M.: 'Distance distributions in finite uniformly random networks: Theory and applications', *IEEE Trans. Veh. Technol.*, 2011, **59**, (2), pp. 940–949
22 Meyer, C.D.: 'Matrix analysis and applied linear algebra' (SIAM publishers, 2001)
23 Van Doorn, E.A., Pollett, P.K.: 'Quasi-stationary distributions for reducible absorbing Markov chains in discrete time', *J. Markov Process. Related Fields*, 2009, **15**, (2), pp. 191–204
24 Langville, A.N., Stewart, W.J.: 'The Kronecker product and stochastic automata networks', *Elsevier J. Comput. Appl. Math.*, 2004, **167**, (2), pp. 429–447
25 Stewart, W.J., Atif, K., Plateau, B.: 'The numerical solution of stochastic automata networks', *Eur. J. Oper. Res.*, 1995, **86**, (3), pp. 503–525

doi: 10.1049/iet-com.2013.0218